# Microscopic origin of the fragile to strong crossover in supercooled water: The role of activated processes

M. De Marzio, G. Camisasca, M. Rovere, and P. Gallo

Citation: The Journal of Chemical Physics **146**, 084502 (2017); doi: 10.1063/1.4975387
View online: http://dx.doi.org/10.1063/1.4975387
View Table of Contents: http://aip.scitation.org/toc/jcp/146/8
Published by the American Institute of Physics

# Microscopic origin of the fragile to strong crossover in supercooled water: The role of activated processes

M. De Marzio, G. Camisasca, M. Rovere, and P. Gallo
*Dipartimento di Matematica e Fisica, Università "Roma Tre," Via della Vasca Navale 84, 00146 Roma, Italy*

(Received 19 September 2016; accepted 20 January 2017; published online 23 February 2017)

We perform an accurate analysis of the density self-correlation functions of TIP4P/2005 supercooled water on approaching the region of the liquid-liquid critical point. In a previous work on this model, we provided evidence of a fragile to strong crossover of the dynamical behavior in the deep supercooled region. The structural relaxation follows the Mode Coupling theory in the fragile region and then deviates from Mode Coupling regime to a strong Arrhenius behavior. This crossover is particularly important in water because it is connected to the thermodynamics of the supercooled region. To better understand the origin of this crossover, we compute now the Van Hove self-correlation functions. In particular we aim at investigating the presence and the role of the hopping phenomena that are the cause of the fragile to strong crossover in simple liquids. In TIP4P/2005 water, we find hopping processes too and we analyze how they depend on temperature and density upon approaching the fragile to strong crossover and the Mode Coupling ideal crossover temperature. Our results show that water behaves like a simple glass former. After an initial ballistic regime, the cage effect dominates the mild supercooled region, with diffusion taking place at long time. At the fragile to strong crossover, we find that hopping (activated) processes start to play a role. This is evidenced by the appearance of peaks in the Van Hove correlation functions. In the deep supercooled regime, our analysis clearly indicates that activated processes dominate the dynamics. The comparison between the Van Hove functions and the radial distribution functions allows one to better understand the mechanism of hopping phenomena in supercooled water and to connect their onset directly with the crossing of the Widom Line. *Published by AIP Publishing.* [http://dx.doi.org/10.1063/1.4975387]

## I. INTRODUCTION

Water plays a relevant role in chemistry, biology, and various technological processes. For this reason many experimental and theoretical studies were conducted to understand its peculiar thermodynamic behavior.[1] Indeed, liquid water displays different kinds of anomalies in all its phase diagrams. The most known of these anomalies is the presence of a temperature of maximum density (TMD), a point where the density measured as function of temperature at constant pressure shows a maximum. At ambient pressure, the TMD is located at 4 °C. The TMD line is the locus of state points of the TMD at different pressures and it separates a region where water behaves as a normal liquid with density increasing at decreasing temperature from a region where density decreases upon cooling. As a consequence, the thermal expansion coefficient also changes its sign across the TMD line.

With refined experimental techniques, water can be maintained in its liquid phase at least down to its temperature of homogeneous nucleation. At ambient pressure, this corresponds to $T \approx -42$ °C. In the supercooled region of liquid water, the interpretation of the very peculiar experimental results is still controversial. Indeed, an anomalous increase of the thermodynamic response functions upon lowering temperature below the melting point has been observed. These functions like the isobaric specific heat and the isothermal compressibility show a power law behavior that can be extrapolated to diverge in the region of deep supercooling at a singular temperature called $T_S$.[2,3] At ambient pressure $T_S \approx -45$ °C.

The anomalous properties of the phase diagram of supercooled water have been interpreted by several possible theoretical scenarios.[4–9] At the heart of the present debate is the Liquid-Liquid Critical Point (LLCP) scenario.[4] In this scenario, the apparent divergences of the thermodynamic response functions are caused by the presence of a second critical point that is the terminal point of a first order phase transition between two liquid phases of supercooled water, a low density liquid (LDL) and a high density liquid (HDL).[10] The presence of a LLCP is difficult to verify experimentally, as the LLCP would be located in the so-called "no-man's land,"[11–13] a thermodynamic region where it is hard to keep water in the metastable liquid phase since nucleation to the stable ice phase prevails. Only recently it was possible to get below the nucleation temperature line with new very sophisticated experimental techniques.[14] It has to be noted that the no-man's land also has a lower border with the region of the amorphous phase of ice, since increasing temperature above the glass transition nucleation to ice prevents the formation of supercooled liquid water.[15]

The LDL and HDL metastable phases are characterized by a different short range order of the water molecules in analogy with the two amorphous ice phases found below the inferior border of no man's land. Indeed, two different phases of glassy water exist, the low density amorphous (LDA) ice and the high density amorphous (HDA) ice,[16–20]

separated by a transition line that appears to be of first order.

In this respect, it is supposed that the extension at higher temperature of this line becomes the coexistence line between the LDL/HDL phases that terminates at the LLCP. The liquid-liquid transition in supercooled water has recently been explained by assuming that the liquid is a mixture of the two forms of water characterized by alternative arrangement of the hydrogen bond network. The phase separation into the LDL/HDL coexistence would be an unmixing entropy driven process taking place at the appropriate thermodynamic conditions.[21–23] Experiments also suggest a bimodal distribution of configurations for water.[14,24–26]

Numerous computational analyses have shown the existence of a LLCP for different water potentials.[4,27–32] More recently further analysis in terms of free energy calculations has confirmed the presence of a LLCP in the ST2 model for water.[33–35] Also the LLCP of the Jagla potential model for water has been rigorously proved to be a second order critical point belonging to the Ising universality class.[36]

Besides the thermodynamic anomalies, the dynamical behavior of water upon supercooling is also a matter of intense studies. In 1996 computer simulation of supercooled SPC/E water[37,38] found that the dynamical behavior can be interpreted in terms of the Mode Coupling Theory (MCT) of glassy dynamics.[39] The MCT predicts that the structural relaxation time of a supercooled liquid asymptotically diverges with a power law upon approaching a temperature $T_C$ that marks the crossover from an ergodic to a non-ergodic regime. It was shown that in supercooled water $T_C$ corresponds to the singular temperature $T_S$. These results were confirmed more recently by spectroscopic[40] and dynamical differential microscopy[41] measurements.

In a number of computer simulations with different model potentials it was confirmed that the dynamics of supercooled water can be interpreted in terms of the MCT. Upon approaching the temperature $T_C$ however the water relaxation dynamics deviates from the fragile MCT behavior and enters in a strong regime. This fragile to strong crossover (FSC) has been found in SPC/E,[42] ST2, TIP5P, and the Jagla model,[43] in TIP4P in bulk and aqueous solutions,[44–47] and recently in TIP4P/2005 bulk water.[48]

The FSC has been related to the presence of a LLCP by considering the Widom line (WL). In critical phenomena this line is defined as the locus of the maxima of the correlation length moving from the critical point into the one phase region.[43,49] The maxima of the response functions are expected to collapse on this single line on approaching the critical point.[43,49–51] By taking into account the properties of the WL emanating from the LLCP, the FSC has been connected to the presence of a liquid-liquid phase transition between a fragile HDL and a strong LDL.[43] We note that a change in dynamics upon crossing the WL has been found also in experiments and simulations of supercritical water[52] and supercritical fluid argon,[53] showing a strong link between dynamics and thermodynamics also in other regions of the phase diagram.

Experiments on confined water that can be more easily cooled avoiding formation of ice show the presence of a FSC[54,55] at the crossing of the WL.[56] These results were also supported by computer simulation of SPC/E water confined in a hydrophilic pore.[57–59] An important feature of glass forming systems, the Boson peak, appears at low temperatures also in water.[60] It has recently been found in nanoconfined water that the Boson peak is also sensitive to the FSC and rises when water is on the strong side of its phase diagram.[61–64]

In the framework of the MCT, the FSC can be interpreted in terms of a crossover to a region where hopping phenomena start to dominate the relaxation dynamics. MCT is mainly based on the idea of the cage effect. Each particle of the fluid at high temperature can diffuse, but upon supercooling it is trapped in a cage of the nearest neighbors and it diffuses when the cage relaxes after a time that becomes longer and longer as the temperature decreases. The temperature $T_C$ marks the transition to a non-ergodic regime where the particles are frozen in their cages. In this respect at $T_C$ the system would undergo structural arrest. In the theory, however, activated processes are neglected. In real systems, in the deep supercooled region when thermal fluctuations are not any more sufficient to dissolve the caging of nearest neighbors, particles can escape from the cage via hopping mechanisms. Consequently, when approaching $T_C$ hopping phenomena start to dominate the dynamics and allow the liquid to rearrange itself also below $T_C$.[39,65] $T_C$ continues to mark the temperature where all cages are frozen. Since hopping processes are activated processes, the dynamics is characterized by an Arrhenius strong behavior. For glass forming systems, hopping phenomena have been examined through the Van Hove Self-Correlation Function (VHSCF) in the Lennard-Jones (LJ) binary mixture[66–69] as connected to deviations from the MCT ideal behavior. In water indications of the presence of hopping as connected to deviation from MCT have been also found.[38,42]

In this paper we inquire more in details on the relation between the FSC and the appearance of the activated hopping processes. Since for supercooled water the fragile to strong transition has been found to occur upon crossing the WL,[43,44,46,48,58] we inquire here to what extent it is also possible to identify the WL as the line that marks the appearance of the hopping processes.

We investigate the presence and the qualitative aspects of hopping phenomena in TIP4P/2005 water in the deep supercooled regime. TIP4P/2005[70] is a popular water potential that reproduces a realistic phase diagram of water both in the stable liquid and in the crystalline phase.[71] A LLCP has been found[32] in the supercooled regime together with an anomalous increase of the thermodynamic response functions.[71] In previous work we found that also for this potential the dynamical behavior of supercooled water can be described in terms of the MCT. We also found that the FSC exists and takes place at the crossing of the WL.[48]

Now through the calculation of the VHSCF, we show that hopping occurs in correspondence of the FSC and therefore upon crossing the WL, and we make a comprehensive analysis of hopping processes upon varying density and temperature.

In Sec. II the simulation details are described. In Sec. III we present the radial VHSCF at the three temporal regimes typical of supercooled liquids and in particular we examine the qualitative and quantitative aspects of the cage regime. In

Sec. IV we show the connection between hopping phenomena and FSC and in Sec. V we investigate hopping at different densities and temperatures, giving new insights for the comprehension of the mechanism underlying these activated processes for water. Sec. VI is devoted to conclusions.

## II. MODEL AND SIMULATION METHODS

In this work we simulated a cubic box of 512 water molecules at three different densities $\rho = 0.95$ g/cm$^3$, $\rho = 0.98$ g/cm$^3$, and $\rho = 1.00$ g/cm$^3$ in the mild and deep supercooled regime. The range of temperature investigated spans from 300 K to 190 K. The interactions between the water molecules are described with the TIP4P/2005 potential.[70] This four-site water potential represents the molecule as composed of two positive charged hydrogens with $q_H = 0.5564\ e$, one neutral oxygen which is a Lennard-Jones (LJ) pole and a negative charged site $M$ with $q_M = -2q_H$ placed along the bisector of the HOH angle and coplanar with the oxygen and hydrogens at distance 0.1546 Å from the oxygen. All the simulations are made with molecular dynamics parallel Gromacs package 4.5.5.[72] A time step of 1 fs was used. We set a LJ cutoff distance of 9.5 Å. We have used the Coulomb interactions, truncated at 9.5 Å, with the Ewald method. In particular the Particle Mesh Ewald (PME) algorithm was used with a Fourier spacing of 1 Å and a fourth degree polynomial. The system has been equilibrated with Berendsen thermostat. The production runs are performed in the NVE ensemble. The longest production runs required 200 ns.

## III. VAN HOVE CORRELATION FUNCTIONS

The dynamics of water in the mild and deep supercooled regime can be studied calculating the oxygen VHSCF $G_S(\mathbf{r}, t)$ (VHSCF), which is defined as

$$G_S(\mathbf{r}, t) = \frac{1}{N}\left\langle \sum_{i=1}^{N} \delta(\mathbf{r} - (\mathbf{r}_O^i(t) - \mathbf{r}_O^i(0)))\right\rangle, \qquad (1)$$

where $N$ is the number of molecules of the system. This function expresses the single particle's probability of being at the position $\mathbf{r}$ with respect to the origin of its trajectory at the time $t$ and provides a detailed description of the average particle evolution in time and space.

In this work we have calculated the radial VHSCF $4\pi r^2 G_S(r, t)$ for the three densities in the range of temperature mentioned in Sec. II. The results for the density $\rho = 1.00$ g/cm$^3$ at $T = 220$ K at different values of time are reported in Fig. 1. The progression of the VHSCF with time reflects the "cage" effect typical of supercooled liquids, as discussed in Ref. 38.

In the figure we also show the same correlator in the (Q,t) space, the Self-Intermediate Scattering Function (SISF) and we mark the time regions spanned by the corresponding VHSCF. At early times, the particle moves ballistically without interacting. In this regime, the VHSCF broadens and its peak lies at larger distances upon increasing time, indicating that the molecule is going away from its original position.

Correspondingly the SISF has an initial fast decay.

In a range of intermediate times, the calculated VHSCFs do not evolve with time and as a consequence they collapse on the same curve. In this time interval, the particle is trapped in a cage formed by its nearest neighbors and is confined in a finite spatial region.

Correspondingly the SISF does not decay and shows a plateau.

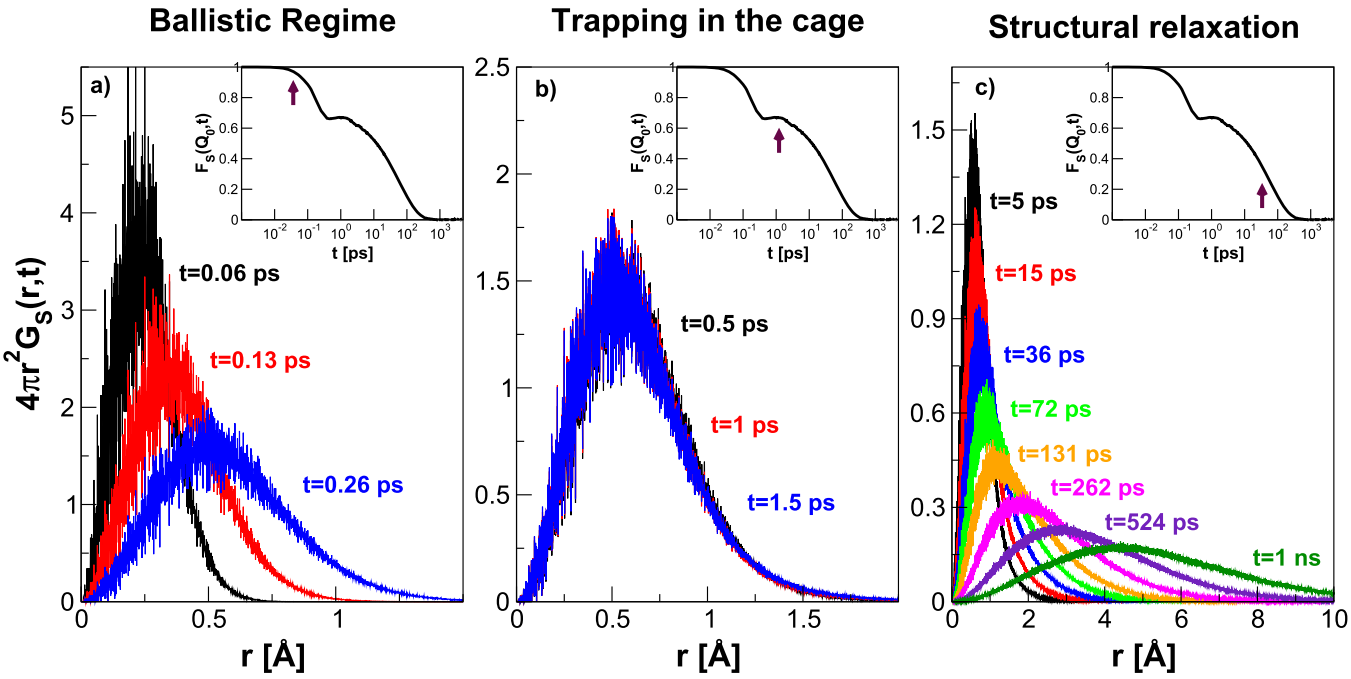


FIG. 1. Radial VHSCF at $T = 220$ K for density $\rho = 1.00$ g/cm$^3$ for various instants of time. The VHSCF is displayed in (a) the ballistic time interval, (b) the intermediate "cage" regime, and (c) the long time diffusive regime. In the insets we plot the same correlator in the (Q, t) space, the Self-Intermediate Scattering Function (SISF). Each arrow marks the time region spanned by the VHSCF of the main panel.

In the range of longer times, longer than 5 ps, the cage dissolves and the particle enters in the diffusive regime, where it explores larger and larger distances showing a VHSCF that spreads with time.

Correspondingly the SISF starts decaying from the plateau and goes to zero for long times. We note that in this region of mild supercooling no extra features appear besides those connected with the cage effect and therefore with a stretched relaxation.

Besides giving a picture of the three regimes typical of supercooled water dynamics, the VHSCF provides information on the particle motion inside the cage. Hypothesizing that the molecule is bound inside the cage by a three-dimensional harmonic potential determined by its interactions with the nearest neighbors, the corresponding VHSCF should have the following Gaussian form:

$$G_S(\mathbf{r},t) = \left(\frac{m\omega^2}{4k_BT\pi}\right)^{3/2} e^{-M\omega^2\mathbf{r}^2/4k_BT}, \qquad (2)$$

where $m$ is the oxygen mass and $\omega$ is the angular frequency of the oscillation. In the range of temperature where the cage effect is more evident and for each of the three densities analyzed we have fitted the radial VHSCF in the cage regime with the radial version of Eq. (2). Fig. 2 shows the result of the fit for $T = 220$ K and $\rho = 1.00$ g/cm$^3$. As already observed in Ref. 38, the VHSCF is successfully fitted by Eq. (2) at distances near the peak but deviates progressively from the Gaussian distribution upon moving away from it. This trend, on the one hand, suggests the harmonic character of the cage confining potential for small oscillations around the center of the cage and on the other hand underlines the importance of anharmonic contributions at larger distances.

From each fit, we have extracted the value of the oscillation frequency $\omega$, whose dependence from density and temperature is plotted in Fig. 3. As we see, the frequency of the oscillation, which is directly related to the elastic constant $k = m\omega^2$ of the harmonic potential, increases upon lowering temperature for each density and decreases with increasing density at fixed temperature. At a certain density, the angular frequency, and therefore the elastic constant $k$, becomes stronger at lower temperatures indicating that the cage is more rigid and binding. At the same time, increasing density isothermally corresponds to, as already shown in Ref. 48, approaching regions where the system relaxes structurally more and more easily. Consequently the cage is less hard and dissolves faster at higher densities, and the respective elastic constant decreases. Upon approaching the corresponding values of the Mode Coupling temperature $T_C$ previously calculated in Ref. 48, the slope of each isochore flattens.

The behavior of the radial VHSCF in the cage regime for a single density is strongly connected to the behavior of the cage radius with temperature. In Fig. 4 the results of the fit of the radial VHSCF to Eq. (2) at several temperatures for $\rho = 1.00$ g/cm$^3$ are displayed. The standard deviation $\sigma$ of the Gaussian distribution of Eq. (2), defined as $\sigma = \sqrt{\frac{2k_BT}{m\omega^2}}$, diminishes at decreasing temperature, and consequently in Fig. 4 the VHSCF becomes narrow and sharp. If we consider the standard deviation as an approximate measure of the particle's mean square

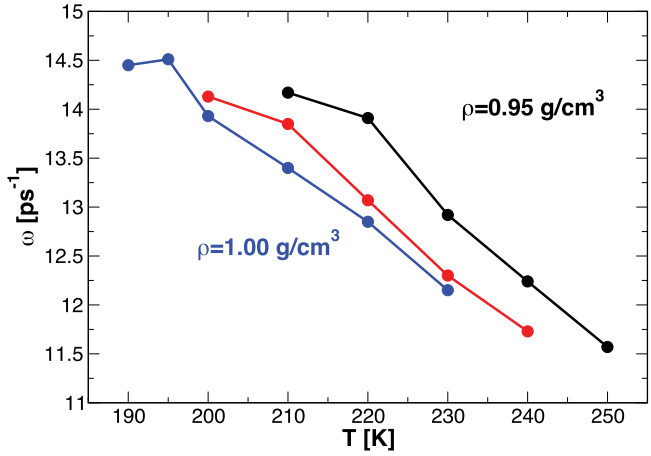


FIG. 3. Values of the angular frequencies obtained by fitting the radial VHSCF with Eq. (2) at the temperature where the cage freezes for longer times the particle motion. Each curve represents one of the three densities investigated, from the lower density $\rho = 0.95$ g/cm$^3$ (black line) to the higher density $\rho = 1.00$ g/cm$^3$ (blue line).

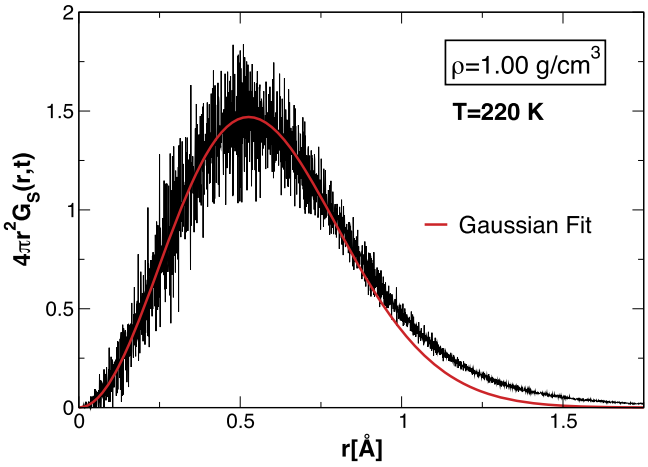


FIG. 2. Radial VHSCF calculated at $T = 220$ K for $\rho = 1.00$ g/cm$^3$. The black data are the MD results and the red line is the fit to Eq. (2).

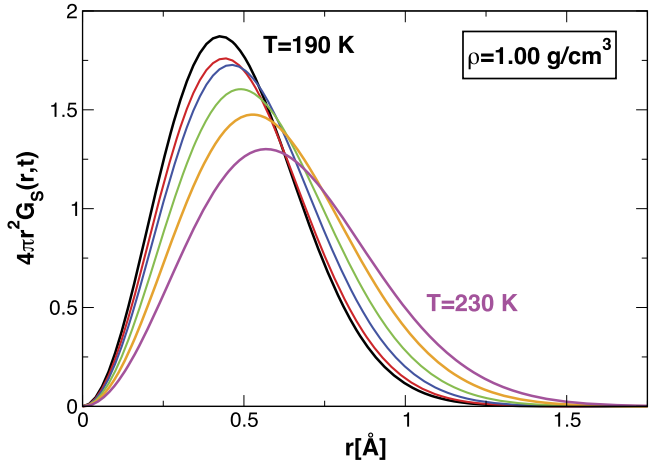


FIG. 4. Fits to Eq. (2) of the radial Van Hove correlation functions at $\rho = 1.00$ g/cm$^3$ at the values of temperatures investigated from $T = 230$ K to $T = 190$ K. For each temperature the VHSCF is computed during the cage time interval.

displacement inside the cage, it means that the cage radius reduces itself by lowering temperature, as predicted by MCT.

## IV. HOPPING PHENOMENA AND FRAGILE TO STRONG CROSSOVER

In the following we explore in detail the VHSCF at long time scale in order to inspect the mechanism through which TIP4P/2005 water relaxes structurally in the deep supercooled regime. In the MCT, the so-called $\alpha$ relaxation process takes place by the diffusion of the particles that, after the cage relaxation, are free to migrate within the liquid, reaching the Brownian regime at long times. In MCT the $\alpha$ relaxation time $\tau$ increases upon lowering temperature as a power law,

$$\tau \sim (T - T_C)^{-\gamma}, \tag{3}$$

where $T_C$ is the Mode Coupling temperature and $\gamma$ is a universal exponent. According to Eq. (3), $T_C$ represents the temperature at which the relaxation time diverges and the system is not able to rearrange itself any more. In the ideal version of the theory where only structural relaxations are taken into account, the cages are frozen and do not break even at longer times, and the system moves from an ergodic phase where it is able to structurally relax to a non-ergodic phase where the dynamics is completely arrested and the system has vitrified.

The MCT prediction of the power law dependence of $\tau$ from temperature is valid for a large range of temperatures and pressures. Nevertheless, real supercooled liquids show the capability to remain ergodic also at temperatures below $T_C$. This is because MCT does not take into account in its ideal formulation the so-called hopping phenomena. Indeed, even if the cage has not dissolved, the particle can escape from it by jumping out and becoming free again to move within the liquid. This activated process, referred as hopping process, restores the ergodicity of the system and introduces a new relaxation mechanism different from the structural relaxation theorized by MCT.

The appearance of hopping phenomena occurs gradually upon lowering temperature. When the system gets close to $T_C$ the $\alpha$ relaxation as predicted by MCT is more and more arduous to realize and hopping begins to dominate the long time scale dynamics. Below $T_C$, the cages are definitely arrested and hopping is the only way for the system to relax. The transition from the MCT diffusion to the hopping mechanism affects the behavior of the translational relaxation time $\tau$ as a function of temperature. The FSC is caused exactly by this transition from the MCT (fragile) power law of Eq. (3) to an exponential Arrhenius (strong) law,

$$\tau = \tau_0 e^{E_A/k_B T}, \tag{4}$$

where $E_A$ is the activation energy. As already shown in Ref. 48, TIP4P/2005 supercooled water has a FSC for all the densities investigated in this work. The values of the Mode Coupling temperatures $T_C$ and the crossover temperatures $T_L$ calculated in Ref. 48 are reported in Table I.

The presence of hopping phenomena in the dynamics of supercooled liquids can be explored through the study of the VHSCF. Indeed, while at higher temperatures the long time regime of the VHSCF shows only the $\alpha$ relaxation, see Fig. 1(c), at sufficiently low temperatures if hopping processes begin to occur one or more weak extra peaks are expected to emerge superposing to the stronger peak of the $\alpha$ relaxation.

TABLE I. Fitting parameters of the MCT Eq. (3) and Arrhenius Eq. (4) for each density and correspondent FSC temperatures as calculated in Ref. 48.

| $\rho$ (g/cm$^3$) | $T_C$ (K) | $\gamma$ | $E_A$ (kJ/mol) | $T_L$ (K) |
|---|---|---|---|---|
| 0.95 | 209.898 | 2.982 | 58.454 | 230 |
| 0.98 | 202.628 | 2.858 | 46.349 | 220 |
| 1.00 | 190.829 | 2.939 | 45.291 | 210 |

In Fig. 5 we present the long time VHSCF for the three densities investigated at three selected values of temperatures. For each density the three temperatures, from left to right, correspond to 10 K above the FSC temperature $T_L$ of that density, 10 K below the $T_L$, and 20 K below the $T_L$. The temperature corresponding to 20 K below the $T_L$ coincides with the MCT temperature $T_C$. The FSC crossover temperature $T_L$ and the MCT temperature $T_C$ are reported in Table I for the densities investigated.

The results of the computation of VHSCF show an overall behavior similar for each density.

At temperature 10 K above the $T_L$, the radial VHSCF decreases and broadens in space when calculated for long times, exhibiting a trend that follows with the asymptotic diffusive motion expected for a liquid following the MCT $\alpha$ relaxation and described in Fig. 1.

By lowering temperature 10 K below the FSC $T_L$, changes occur in the VHSCF, as shown in the second panel of each density in Fig. 5. On the one hand, the peak of the distribution remains blocked at a fixed position even at long times showing that with a certain probability the particle is still trapped in the cage. On the other hand, a weak second peak begins to rise at longer times, deforming the typical trend of the $\alpha$ relaxation distribution. This can be seen, for example, in the VHSCF at 1 ns for $\rho = 0.95$ g/cm$^3$ in the second panel.

The second peak reveals that hopping phenomena begin to appear.

By further cooling the system down to $T_C$ (third panels of Fig. 5), the hopping peaks become clearly visible as shoulders in the VHSCF (see 8 ns, 10 ns, and 34 ns, respectively, for $\rho = 0.95$ g/cm$^3$, $\rho = 0.98$ g/cm$^3$, and $\rho = 1.00$ g/cm$^3$). At this temperature, the cages are completely frozen and particles can escape from them only via hopping processes which dominate totally the dynamics.

It should be noticed that, upon lowering temperature, the VHSCF with the same height of the peak correspond to longer times, indicating that the liquid capability to rearrange itself is reduced.

We also stress that, as stated in the Introduction, we already showed in a previous paper that the FSC crossover coincides with the WL which is the locus of the maxima of the correlation length in the one phase region above the LLCP. This points to a strong relation between dynamics and thermodynamics in water.

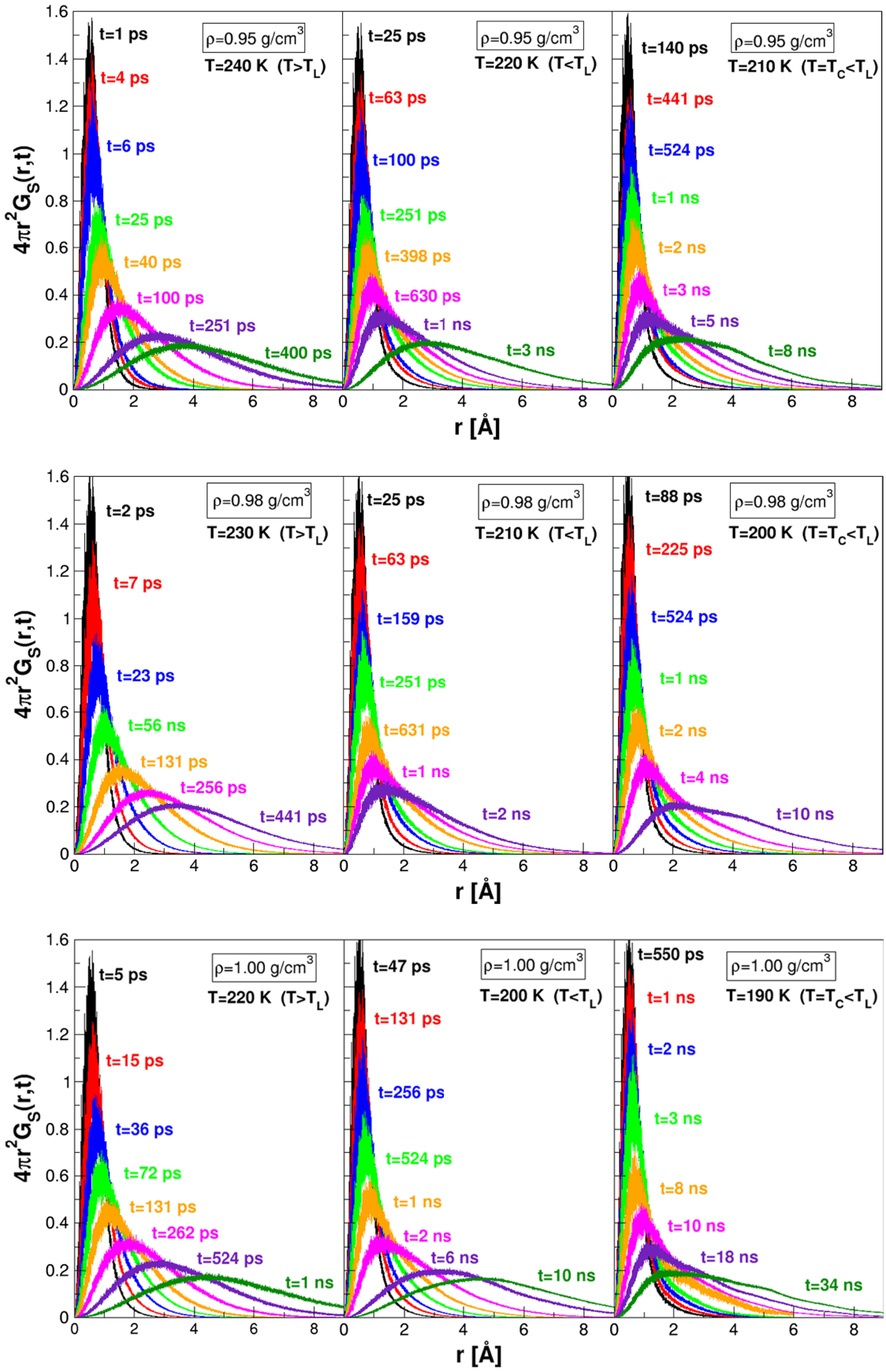


FIG. 5. Radial VHSCF in the long time diffusive regime calculated for three densities. The top row corresponds to $\rho = 0.95$ g/cm$^3$, the central row to $\rho = 0.98$ g/cm$^3$, and the bottom row to $\rho = 1.00$ g/cm$^3$. For each density, the VHSCF is shown from left to right, for temperatures that correspond to 10 K above the FSC temperature $T_L$ of that density, 10 K below the $T_L$ of that density, and 20 K below the $T_L$ of that density. The temperature corresponding to 20 K below the $T_L$ coincides with the MCT temperature $T_C$ for all densities. The FSC crossover temperature $T_L$ and the MCT temperature $T_C$ are reported in Table I for the densities investigated.

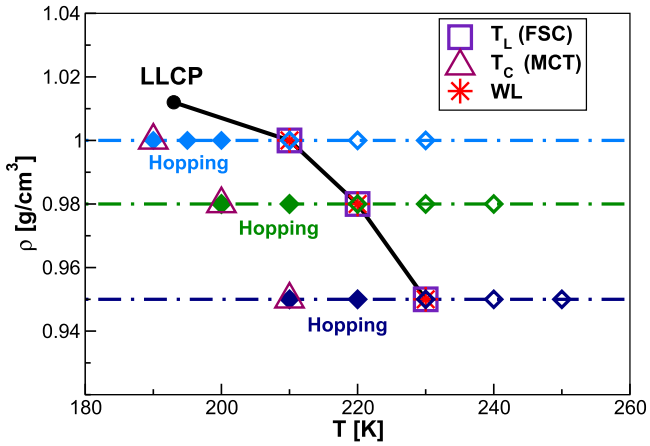


FIG. 6. $\rho$T thermodynamic plane. We plot in the figure the LLCP location,[32] the $T_L$ line, the WL, and the MCT $T_C$ values.[48] We also show the isochores investigated and indicate in empty diamonds the state points where hopping is absent and in filled diamonds the state points where hopping is present. It is clear from the picture that hopping is present below the FSC line which coincides with the WL.

In order to better locate the crossovers and the WL in the $\rho$T plane we have plotted in Fig. 6 the FSC $T_L$, the WL, the LLCP, and the MCT $T_C$ for all densities investigated. We also plotted for each isochore all the state points investigated distinguishing those whose VHSCF shows hopping from those whose VHSCF does not show it. As it can be clearly seen, there are no hopping phenomena above $T_L$ while these phenomena intervene when the system passes the respective FSC temperature $T_L$. The ideal MCT $T_C$ line falls in a region where hopping processes are already present. This happens also for other glass formers. Hopping starts to show up before all cages are frozen. At $T_C$ hopping dominates as all cages are structurally arrested. In water we have a further important event which is the presence of a peculiar thermodynamics related to a critical phenomenon and therefore the presence of a WL.

Our analysis represents a strong confirmation that the FSC observed in Ref. 48 is generated by the activation of hopping processes that are more favored where water is less dense, i.e., below the WL therefore in the region of the liquid which is more LDL-like.

## V. HOPPING PHENOMENA AND RADIAL DISTRIBUTION FUNCTIONS (RDFs)

In order to better study the mechanism at the basis of hopping processes, we now analyze the VHSCF at very long times for each of the densities investigated. For long times, hopping phenomena reach a statistics large enough to make hopping peaks more pronounced and visible. In Fig. 7 we plot the VHSCF together with the oxygen-oxygen Radial Distribution Function (RDF) $g_{OO}(r)$ computed for the three densities at their Mode Coupling temperature $T_C$. The $g_{OO}(r)$ are rescaled by a factor in order to make easier the comparison. Fig. 7 shows clearly that hopping is the dominant process at $T_C$ and provides a picture of the evolution of hopping phenomena with time.

Let us remind that according to the ideal version of MCT at $T_C$ all cages are frozen. By looking at the black curves, we first of all notice that after a long time the particle has indeed not moved much compared to the typical MCT evolution shown in Fig. 1 after the breaking of the cage. The black curve of each panel of Fig. 7 therefore still represents the probability distribution of a particle that has a great chance of staying trapped in the frozen cage as its peak corresponds to a distance roughly within the cage radius. At longer times the other curves

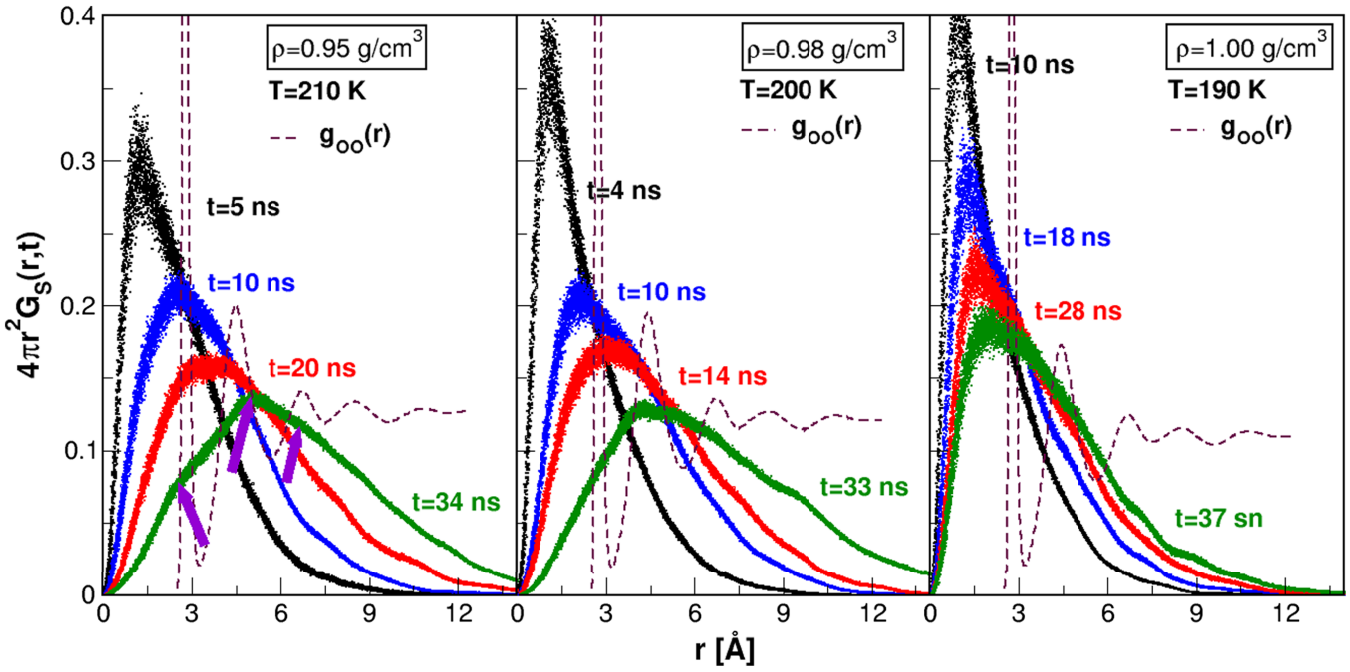


FIG. 7. Radial VHSCF in the long time diffusive regime calculated for $\rho$ = 0.95 g/cm$^3$, $\rho$ = 0.98 g/cm$^3$, $\rho$ = 1.00 g/cm$^3$. For each density, the VHSCF is shown at $T = T_C$, with $T_C$ the respective Mode Coupling temperature reported in Table I. The $g_{OO}(r)$ at $T_C$ are also reported and rescaled to make the comparison more clear. In the first panel arrows mark the exact position of the hopping peaks at $t$ = 34 ns.

show that the particle starts to hop out of the cage with a probability that becomes larger and larger when increasing time as witnessed by the decrease of intensity of the curve in correspondence with the cage radius. The particle first hops to the closest empty spaces that can be found in correspondence of the first peak of the oxygen-oxygen RDF and then, for longer times, the probability to hop also to further energetically favorable empty spaces becomes different from zero. And this is evident because for longer times, in spite of the fact that a probability to remain in the cage is left, multiple peaks begin to emerge in the probability distribution function in correspondence to the other peaks of the $g_{OO}(r)$. At longer times, these further peaks grow and become more pronounced. This means that, upon increasing time, particles explore greater distances, jumping consecutively from one shell to the following. In principle, hopping peaks should increase and decrease their height remaining locked in correspondence to the peaks of the RDF. Nevertheless, Fig. 7 displays a slight shift of the peaks of the VHSCF at very long times. We also showed in the first panel the exact location of the hopping peaks. Considering that all the arrows correspond circa to a peak of the RDF, but that the displacement between the location of the hopping feature in the VHSCF and the peak of the RDF appears to be random, the slight displacements that we observe could be due to statistics issues.

It should be noticed that comparing the VHSCF of the same heights, which corresponds to analyze the same relative times in the system dynamics, hopping appears to be more favored at lower densities. Indeed, at $t = 10$ ns and $\rho = 0.95$ g/cm$^3$ the hopping peak relative to the first shell of $g_{OO}(r)$ is the dominant peak and the "cage" peak is weak and lower, while at $t = 28$ ns and $\rho = 1.00$ g/cm$^3$ the "cage" peak is still the higher peak and hopping peaks are small. This suggests that, even if all the densities are studied at their relative $T_C$, the activation of hopping processes occurs more easily and rapidly at lower densities.

In Fig. 8 we plot the long time VHSCF for the three densities at $T = 210$ K. The comparison of VHSCF at different densities shows that curves with the same height correspond to times that are longer at decreasing density. This aspect is a direct consequence of water's diffusion anomaly,[42,71,73–76] already observed in Ref. 48 through the study of the SISF, for which lower densities coincide with structures with less mobility and slower dynamics.

The frequency and intensity with which hopping phenomena occur are a measure of how much hopping is favored for each density. We can see from Fig. 8 that at the same temperature there is a monotonic behavior of the hopping strength with density. The relative sharpness and intensity of the hopping peaks grow upon decreasing density. At $\rho = 0.95$ g/cm$^3$, hopping peaks are well visible and sharp. Upon increasing density, hopping phenomena reduce their intensity and frequency, as shown at $\rho = 0.98$ g/cm$^3$ and $\rho = 1.00$ g/cm$^3$ where the peaks are progressively smoother and less detectable. This trend is again a confirmation of the interpretation of hopping phenomena as the cause of the FSC. At fixed temperature, higher densities are farther from their respective $T_C$ than lower densities. Indeed, increasing density isothermally corresponds to moving away from the region where hopping is the dominant dynamical process and getting closer to the phase where $\tau(T)$ is still well described by Eq. (3). The fact that hopping is favored where water is less dense directly connects to the fact that in water the FSC was found upon crossing the WL. Indeed this line separates two regions where, respectively, HDL or LDL structures are more favored. Therefore, this further confirms that, upon crossing the WL, hopping becomes more favored as water goes on the side of the WL where it is less dense and consequently the dynamics crosses from fragile to strong.

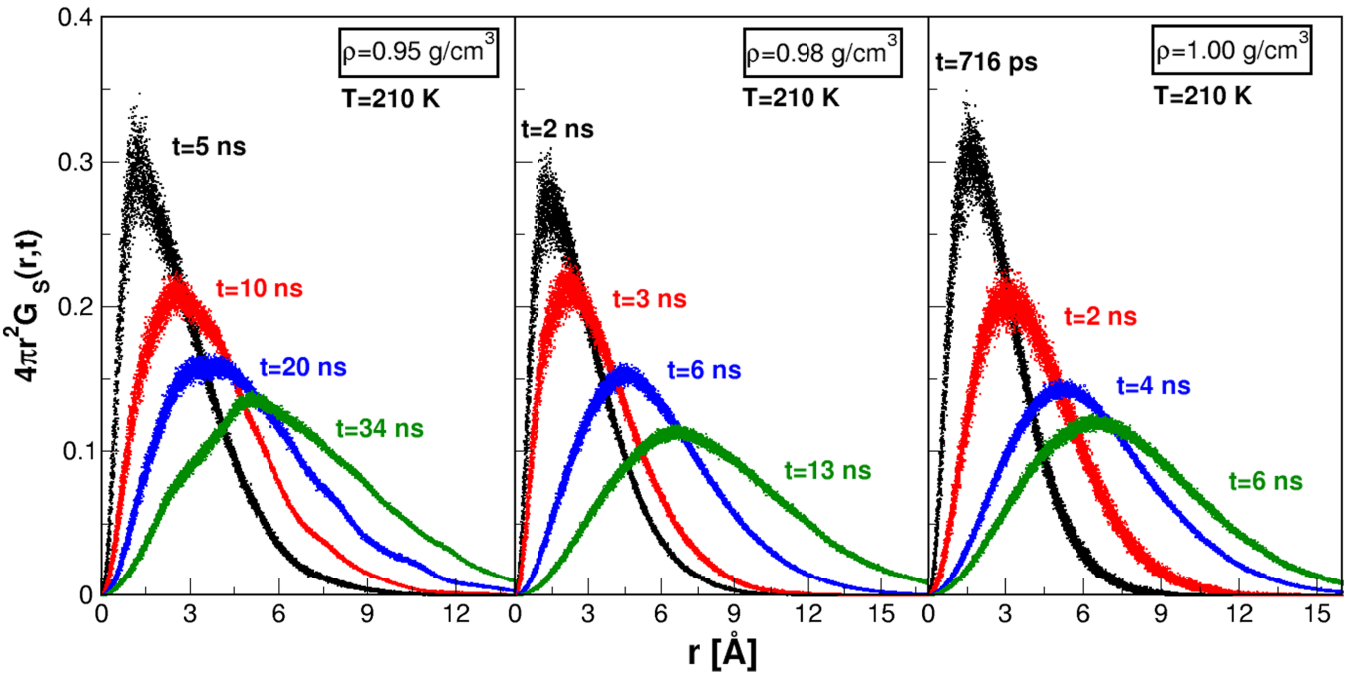


FIG. 8. Radial VHSCF in the long time diffusive regime calculated for $\rho = 0.95$ g/cm$^3$, $\rho = 0.98$ g/cm$^3$, $\rho = 1.00$ g/cm$^3$ at the same temperature $T = 210$ K.

## VI. CONCLUSIONS

In this paper we have analyzed the dynamical behavior of supercooled TIP4P/2005 water through the computation of VHSCF for different densities and we have examined the connections between the hopping phenomena, the FSC, and the WL. Our results show that in the mild supercooled region the dynamics of TIP4P/2005 exhibits the typical cage effect of supercooled liquids. As a function of time after the initial ballistic regime, the intermediate transient cage regime takes place before the final diffusive regime. The VHSCF in the cage regime suggests a possible harmonic character of the confining potential with an elastic constant stronger and stronger at lower temperatures and densities. For all the densities investigated, at temperatures near the respective Mode Coupling temperature $T_C$ the VHSCF shape changes progressively and new features appear besides the diffusive shape.

Crossing the FSC, a weak hopping peak arises and becomes more evident and sharp at lower temperatures. This phenomenon is clear evidence of the connection between the FSC and the occurrence of hopping processes as the relaxation process in deep supercooled regime. At $T_C$ the VHSCF shows that structural relaxation through the cage breaking is not more possible and activated hopping processes dominate the dynamics. When this happens, multiple peaks appear in correspondence of the peaks of the oxygen-oxygen RDF revealing that the particles escape from the cage and jump consecutively from one shell to another at greater distance. Compared to the Lennard-Jones binary mixtures,[67–69] the hopping peaks in TIP4P/2005 are less clear and visible and this is probably due to the molecular character of liquid water, leading to a steric hindrance. Moreover, an analysis with respect to density shows that hopping is more favored at lower densities, where the system is more structurally ordered and has less mobility. These results show that the LDL phase of water is characterized by a strong dynamics and the WL separates the fragile regime on the HDL side from the strong regime on the LDL side regime.

The interpretation of the anomalies of supercooled water is still the matter of a vivid debate.[1] We expect that improved experimental techniques would be able to shed more light on water in approaching its glass transition and to test the theoretical approaches and hypothesis. It is particularly relevant to understand how the presence of the hypothesized LLCP and the coexistence between the two LDL/HDL phases can determine the peculiar properties of water and it is essential in this respect to connect thermodynamics with the dynamic behavior. The fact that the dynamics of supercooled water can be interpreted in terms of the MCT was a breakthrough in the theoretical understanding of the water dynamics.[37,38] The FSC and its relation with the thermodynamics of supercooled water through the WL can be also interpreted in terms of MCT and hopping effects.

Hopping is a phenomenon expected for many glass formers but it has been very poorly studied in molecular liquids like water. So it is very important to show how hopping features develop in molecular liquids. Besides, in water the complex thermodynamic features and the slow dynamics mutually influence each other. The aim of the present analysis has been to determine the precise evolution of the relaxation dynamics of water from the MCT regime to the hopping dominated regime. To conclude, all the aspects of the cage regime and hopping phenomena found in our simulations confirm hopping as the cause of the FSC in water and link its rise to the crossing of the WL, being that hopping is more favored where water is less dense.


[1] P. Gallo, K. Amann-Winkel, C. A. Angell, M. A. Anisimov, F. Caupin, C. Chakravarty, E. Lascaris, T. Loerting, A. Z. Panagiotopoulos, J. Russo, J. A. Sellberg, H. E. Stanley, H. Tanaka, C. Vega, L. Xu, and L. G. M. Pettersson, Chem. Rev. **116**, 7463 (2016).
[2] R. J. Speedy and C. A. Angell, J. Chem. Phys. **65**, 851 (1976).
[3] V. Holten, C. E. Bertrand, M. A. Anisimov, and J. V. Sengers, J. Chem. Phys. **136**, 094507 (2012).
[4] P. H. Poole, F. Sciortino, U. Essmann, and H. E. Stanley, Nature **360**, 324 (1992).
[5] S. Sastry, P. G. Debenedetti, F. Sciortino, and H. E. Stanley, Phys. Rev. E **53**, 6144 (1996).
[6] R. P. Rebelo, P. G. Debenedetti, and S. Sastry, J. Chem. Phys. **109**, 626 (1998).
[7] P. G. Debenedetti, J. Phys.: Condens. Matter **15**, R1669 (2003).
[8] G. Pallares, M. E. M. Azouzi, M. A. Gonzalez, J. L. Aragones, J. L. F. Abascal, C. Valeriani, and F. Caupin, Proc. Natl. Acad. Sci. U. S. A. **111**, 7936 (2014).
[9] C. A. Angell, Science **319**, 582 (2008).
[10] A. Nilsson and L. G. M. Pettersson, Chem. Phys. **389**, 1 (2011).
[11] H. E. Stanley, MRS Bull. **24**, 22 (1999).
[12] O. Mishima and H. E. Stanley, Nature **392**, 164 (1998).
[13] O. Mishima and H. E. Stanley, Nature **396**, 329 (1998).
[14] J. A. Sellberg, C. Huang, T. A. McQueen, N. D. Loh, H. Laksmono, D. Schlesinger, R. G. Sierra, D. Nordlund, C. Y. Hampton, D. Starodub, D. P. DePonte, M. Beye, C. Chen, A. V. Martin, A. Barty, K. T. Wikfeldt, T. M. Weiss, C. Caronna, J. Feldkamp, L. B. Skinner, M. M. Seibert, M. Messerschmidt, G. J. Williams, S. Boutet, L. G. M. Pettersson, M. J. Bogan, and A. Nilsson, Nature **510**, 381 (2014).
[15] K. Amann-Winkel, R. Boehmer, F. Fujara, C. Gainaru, B. Geil, and T. Loerting, Rev. Mod. Phys. **88**, 011002 (2016).
[16] O. Mishima, L. D. Calvert, and E. Whalley, Nature **314**, 76 (1985).
[17] K. Winkel, M. Elsaesser, E. Mayer, and T. Loerting, J. Chem. Phys. **128**, 044510 (2008).
[18] C. U. Kim, B. Barstow, M. V. Tate, and S. M. Gruner, Proc. Natl. Acad. Sci. U. S. A. **106**, 4596 (2009).
[19] K. Winkel, E. Mayer, and T. Loerting, J. Phys. Chem. B **115**, 14141 (2011).
[20] S. Klotz, T. Strässle, R. Nelmes, J. Loveday, G. Hamel, G. Rousse, B. Canny, J. Chervin, and A. Saitta, Phys. Rev. Lett. **94**, 025506 (2005).
[21] V. Holten and M. Anisimov, Sci. Rep. **2**, 713 (2012).
[22] H. Tanaka, Phys. Rev. Lett. **80**, 5750 (1998).
[23] R. S. Singh, J. W. Biddle, P. G. Debenedetti, and M. A. Anisimov, J. Chem. Phys. **144**, 144504 (2016).
[24] A. Taschin, P. Bartolini, R. Eramo, R. Righini, and R. Torre, Nat. Commun. **4**, 2401 (2013).
[25] C. Huang, K. T. Wikfeldt, T. Tokushima, D. Nordlund, Y. Harada, U. Bergmann, M. Niebuhr, T. M. Weiss, Y. Horikawa, M. Leetmaa, M. P. Ljungberg, O. Takahashi, A. Lenz, L. Ojamae, A. P. Lyubartsev, S. Shin, L. G. M. Pettersson, and A. Nilsson, Proc. Natl. Acad. Sci. U. S. A. **106**, 15214 (2009).
[26] T. Tokushima, Y. Harada, O. Takahashi, Y. Senba, H. Ohashi, L. G. M. Pettersson, A. Nilsson, and S. Shin, Chem. Phys. Lett. **460**, 387 (2008).
[27] S. Harrington, P. H. Poole, F. Sciortino, and H. E. Stanley, J. Chem. Phys. **107**, 7443 (1997).
[28] M. Yamada, S. Mossa, H. Stanley, and F. Sciortino, Phys. Rev. Lett. **88**, 195701 (2002).
[29] P. H. Poole, I. Saika-Voivod, and F. Sciortino, J. Phys.: Condens. Matter **17**, L431 (2005).
[30] D. Paschek, Phys. Rev. Lett. **94**, 217802 (2005).
[31] D. Corradini, M. Rovere, and P. Gallo, J. Chem. Phys. **132**, 134508 (2010).
[32] J. L. F. Abascal and C. Vega, J. Chem. Phys. **133**, 234502 (2010).
[33] J. Palmer, R. Car, and P. Debenedetti, Faraday Discuss. **167**, 77 (2013).
[34] J. Palmer, F. Martelli, Y. Liu, R. Car, A. Z. Panagiotopoulos, and P. G. Debenedetti, Nature **510**, 385 (2014).
[35] P. H. Poole, R. K. Bowles, I. Saika-Voivod, and F. Sciortino, J. Chem. Phys. **138**, 034505 (2013).

[36]P. Gallo and F. Sciortino, Phys. Rev. Lett. **109**, 177801 (2012).
[37]P. Gallo, F. Sciortino, P. Tartaglia, and S.-H. Chen, Phys. Rev. Lett. **76**, 2730 (1996).
[38]F. Sciortino, P. Gallo, P. Tartaglia, and S.-H. Chen, Phys. Rev. E **54**, 6331 (1996).
[39]W. Götze, *Complex Dynamics of Glass-Forming Liquids: A Mode-Coupling Theory* (Oxford University Press, Oxford, 2009).
[40]R. Torre, P. Bartolini, and R. Righini, Nature **428**, 296 (2004).
[41]A. Dehaoui, B. Issenmann, and F. Caupin, Proc. Natl. Acad. Sci. U. S. A. **112**, 12020 (2015).
[42]F. W. Starr, F. Sciortino, and H. E. Stanley, Phys. Rev. E **60**, 6757 (1999).
[43]L. Xu, P. Kumar, S. V. Buldyrev, S. H. Chen, P. H. Poole, F. Sciortino, and H. E. Stanley, Proc. Natl. Acad. Sci. U. S. A. **102**, 16558 (2005).
[44]P. Gallo and M. Rovere, J. Chem. Phys. **137**, 164503 (2012).
[45]D. Corradini, S. V. Buldyrev, P. Gallo, and H. E. Stanley, Phys. Rev. E **81**, 061504 (2010).
[46]P. Gallo, D. Corradini, and M. Rovere, J. Chem. Phys. **139**, 204503 (2013).
[47]D. Corradini, P. Gallo, S. V. Buldyrev, and H. E. Stanley, Phys. Rev. E **85**, 051503 (2012).
[48]M. De Marzio, G. Camisasca, M. Rovere, and P. Gallo, J. Chem. Phys. **144**, 074503 (2016).
[49]G. Franzese and H. E. Stanley, J. Phys.: Condens. Matter **19**, 205126 (2007).
[50]D. Fuentevilla and M. Anisimov, Phys. Rev. Lett. **97**, 195702 (2006).
[51]J. Luo, L. Xu, E. Lascaris, H. E. Stanley, and S. V. Buldyrev, Phys. Rev. Lett. **112**, 135701 (2014).
[52]P. Gallo, D. Corradini, and M. Rovere, Nat. Commun. **5**, 5806 (2014).
[53]G. Simeoni, T. Bryk, F. Gorelli, M. Krisch, G. Ruocco, M. Santoro, and T. Scopigno, Nat. Phys. **6**, 503 (2010).
[54]A. Faraone, L. Liu, C.-Y. Mou, C.-W. Yen, and S.-H. Chen, J. Chem. Phys. **121**, 10843 (2004).
[55]L. Liu, S.-H. Chen, A. Faraone, C.-W. Yen, and C.-Y. Mou, Phys. Rev. Lett. **95**, 117802 (2005).
[56]Y. Zhang, M. Lagi, E. Fratini, P. Baglioni, E. Mamontov, and S.-H. Chen, Phys. Rev. E **79**, 040201 (2009).
[57]P. Gallo, M. Rovere, and S.-H. Chen, J. Phys. Chem. Lett. **1**, 729 (2010).
[58]P. Gallo, M. Rovere, and S.-H. Chen, J. Phys.: Condens. Matter **24**, 064109 (2012).
[59]P. Gallo, M. Rovere, and S.-H. Chen, J. Phys.: Condens. Matter **22**, 284102 (2010).
[60]F. Venturini, P. Gallo, M. Ricci, A. Bizzarri, and S. Cannistraro, J. Chem. Phys. **114**, 10010 (2001).
[61]P. Kumar, K. T. Wikfeldt, D. Schlesinger, L. G. M. Pettersson, and H. E. Stanley, Sci. Rep. **3**, 1980 (2013).
[62]Z. Wang, K.-H. Liu, P. Le, M. Li, W.-S. Chiang, J. B. Leao, J. R. D. Copley, M. Tyagi, A. Podlesnyak, A. I. Kolesnikov, C.-Y. Mou, and S.-H. Chen, Phys. Rev. Lett. **112**, 237802 (2014).
[63]Z. Wang, A. I. Kolesnikov, K. Ito, A. Podlesnyak, and S.-H. Chen, Phys. Rev. Lett. **115**, 235701 (2015).
[64]A. Cupane, M. Fomina, and G. Schiro, J. Chem. Phys. **141**, 18C510 (2014).
[65]W. Götze and L. Sjögren, Transp. Theory Stat. Phys. **24**, 801 (1995).
[66]P. Gallo, R. Pellarin, and M. Rovere, Europhys. Lett. **57**, 212 (2002).
[67]P. Gallo, R. Pellarin, and M. Rovere, Phys. Rev. E **67**, 041202 (2003).
[68]P. Gallo, A. Attili, and M. Rovere, Phys. Rev. E **80**, 061502 (2009).
[69]A. Attili, P. Gallo, and M. Rovere, J. Chem. Phys. **123**, 174510 (2005).
[70]J. L. F. Abascal and C. Vega, J. Chem. Phys. **123**, 234505 (2005).
[71]H. L. Pi, J. L. Aragones, C. Vega, E. G. Noya, J. L. F. Abascal, M. A. Gonzalez, and C. McBride, Mol. Phys. **107**, 365 (2009).
[72]B. Hess, C. Kutzner, D. V. der Spoel, and E. Lindahl, J. Chem. Theory Comput. **4**, 435 (2008).
[73]C. Angell, E. Finch, and P. Bach, J. Chem. Phys. **65**, 3063 (1976).
[74]F. Prielmeier, E. Lang, R. Speedy, and H.-D. Lüdemann, Phys. Rev. Lett. **59**, 1128 (1987).
[75]A. Scala, F. W. Starr, E. La Nave, F. Sciortino, and H. E. Stanley, Nature **406**, 166 (2000).
[76]J. R. Errington and P. G. Debenedetti, Nature **409**, 318 (2001).